

ASSESSING RADIATION PRESSURE AS A FEEDBACK MECHANISM IN STAR-FORMING GALAXIES

BRETT H. ANDREWS¹ & TODD A. THOMPSON^{1,2,3}

SUBMITTED TO APJ

ABSTRACT

Radiation pressure from the absorption and scattering of starlight by dust grains may be an important feedback mechanism in regulating star-forming galaxies. We compile data from the literature on star clusters, star-forming subregions, normal star-forming galaxies, and starbursts to assess the importance of radiation pressure on dust as a feedback mechanism, by comparing the luminosity and flux of these systems to their dust Eddington limit. This exercise motivates a novel interpretation of the Schmidt Law, the $L_{\text{IR}}-L'_{\text{CO}}$ correlation, and the $L_{\text{IR}}-L'_{\text{HCN}}$ correlation. In particular, the linear $L_{\text{IR}}-L'_{\text{HCN}}$ correlation is a natural prediction of radiation pressure regulated star formation. Overall, we find that the Eddington limit sets a hard upper bound to the luminosity of any star-forming region. Importantly, however, many normal star-forming galaxies have luminosities significantly below the Eddington limit. We explore several explanations for this discrepancy, especially the role of “intermittency” in normal spirals—the tendency for only a small number of subregions within a galaxy to be actively forming stars at any moment because of the time-dependence of the feedback process and the luminosity evolution of the stellar population. If radiation pressure regulates star formation in dense gas, then the gas depletion timescale is 6 Myr, in good agreement with observations of the densest starbursts. Finally, we highlight the importance of observational uncertainties—namely, the dust-to-gas ratio and the CO-to-H₂ and HCN-to-H₂ conversion factors—that must be understood before a definitive assessment of radiation pressure as a feedback mechanism in star-forming galaxies.

Subject headings: galaxies: general, evolution, ISM, stellar content, starburst — stars: formation

1. INTRODUCTION

Understanding global star formation is crucial in understanding galaxy evolution and the assembly of the $z = 0$ stellar population over cosmic time. Observations indicate that only a few percent of the available gas reservoir in galaxies is converted into stars per local free-fall time (Kennicutt 1998; Krumholz & Tan 2007). In addition, models of the interstellar medium (ISM) suggest that energy and momentum injected by massive stars could act as a feedback loop by driving supersonic turbulence, which would cause most of the gas to be insufficiently dense to collapse, rendering star formation inefficient (Krumholz & McKee 2005). However, the interaction between star formation and the ISM is not well understood, and a mechanism for the regulation of star formation across the large dynamic range of star-forming environments has not yet been conclusively identified. Proposed mechanisms include supernova explosions, expanding HII regions, stellar winds, cosmic rays, magnetic fields, and radiation pressure on dust (McKee & Ostriker 1977; Matzner 2002; Cunningham 2008; Chevalier & Fransson 1984; Socrates et al. 2008; Kim 2003; Scoville et al. 2001; Scoville 2003; Thompson, Quataert, & Murray 2005, hereafter TQM; Krumholz & Matzner 2009, hereafter KM09; Murray, Quataert, & Thompson 2010, hereafter MQT; Draine 2010; Hopkins et al. 2010).⁴

In the case of radiation pressure on dust, UV and optical radiation from OB stars is absorbed and scattered by dust grains and subsequently re-radiated as IR radiation. The dust grains are coupled to the gas of the ISM through collisions

and magnetic fields, so radiation pressure on the dust exerts a force on the gas as well (O’dell et al. 1967; Ferrara 1993; Laor & Draine 1993; Murray, Quataert, & Thompson 2005). On galaxy scales, TQM showed that radiation pressure could constitute the majority of the vertical pressure support in dense starburst galaxies such as ultra-luminous infrared galaxies (ULIRGs). Likewise, models of giant molecular cloud (GMC) disruption predict that radiation pressure is the dominant feedback mechanism regulating star formation in the birth of massive star clusters (MQT; KM09). In this picture, gas in a marginally-stable galactic disk collapses to form a GMC and a central compact star cluster. When the stellar mass and luminosity of the cluster exceed the Eddington limit for dust, the overlying gas reservoir is expelled. Thus, the final stellar mass in individual star clusters is regulated by the dust Eddington limit. The centers of ULIRGs and GMC cores are optically thick to both UV and the re-radiated IR photons, which make them ideal candidates for radiation pressure support since essentially all of the momentum from the starlight is efficiently transferred to the gas. Recent observations indicate that the most luminous GMCs in the Milky Way are disrupted by radiation pressure (Murray 2010).

In this paper, we critically assess the theory of radiation pressure regulated star formation by comparing the picture developed by TQM, MQT, and KM09 with the available observations of star-forming galaxies ranging from dense individual star clusters and GMCs, to normal spiral galaxies and starbursts. In §2 we describe the current model of radiation pressure feedback. We emphasize the deviations from the simplest version of the dust Eddington limit in assessing radiation pressure regulated feedback that arise from ambiguities in the value of the flux-mean dust opacity, and the tendency for low-density galaxies to have highly intermittent knots or hotspots of star formation across their disks. In §3, we compare data from the literature to models of radiative feedback. In §4, we discuss our conclusions, the major observational

¹ Department of Astronomy, The Ohio State University, 140 West 18th Avenue, Columbus, OH 43210, andrews@astronomy.ohio-state.edu

² Center for Cosmology and Astroparticle Physics, The Ohio State University, 191 West Woodruff Avenue, Columbus, OH 43210.

³ Alfred P. Sloan Fellow

⁴ ISM turbulence driven by non-stellar processes, such as disk instabilities, has also been proposed (Sellwood & Balbus 1999; Wada et al. 2002; Piontek & Ostriker 2004, 2007).

and theoretical uncertainties in our analysis, and the implications of our results.

2. THEORETICAL ELEMENTS

The statement that radiation pressure may be an important feedback mechanism in galaxies is equivalent to the statement that galaxies as a whole or the star-forming subregions within them approach or exceed the Eddington limit for dust,

$$F_{\text{Edd}} = \frac{4\pi Gc\Sigma}{\kappa_{\text{F}}}, \quad (1)$$

where F_{Edd} is the Eddington flux, Σ is the surface density of the dominant component of gravitational potential in the star-forming region, and κ_{F} is the flux-mean opacity. The overall picture is that star-forming regions meet the Eddington limit and self-regulate in analogy with an individual massive star (TQM; see also Scoville et al. 2001; Scoville 2003; MQT; KM09). We would thus naively expect to test the theory of radiation pressure regulated star formation by taking the ratio of the observed flux (F_{obs}) to F_{Edd} . However, a direct comparison between the simple theoretical expectation

$$F_{\text{obs}}/F_{\text{Edd}} \rightarrow 1 \quad (2)$$

and the observations is complicated by both theoretical and observational uncertainties. For example, although gas is expected to be the dominant mass component in and around massive star clusters in formation, it is unclear how best to estimate Σ in equation (1) for unresolved galaxies or unresolved star-forming subregions. Below, we consider both CO and HCN emission (see §3; Figures 1 & 2), but the conversion from the luminosity in either of these molecular gas tracers to gas mass where the stars are forming, is highly uncertain. Another uncertainty is the coupling of the radiation field to the gas, which is complicated due to both the non-gray nature of the dust opacity and the clumpiness of the gas on all scales (see §2.1 below). Finally, there is an additional complication not readily apparent from the time-independent statement of equation (2): the star formation rate (SFR) across the face of a large spiral galaxy is highly intermittent so that only a small number of subregions are bright at any time. As discussed by MQT and in detail below (§2.2), this *intermittency* can cause normal star-forming galaxies to appear significantly sub-Eddington ($F_{\text{obs}}/F_{\text{Edd}} \ll 1$) when only their average properties are considered, but much closer to Eddington when a model is used to take this effect into account.

2.1. The Radiation Pressure Force

The coupling between radiation and gas in star-forming environments is complex primarily because the flux-mean opacity κ_{F} in equation (1) has a full range of more than 3 dex, depending on whether the SED of the system considered is dominated by UV or FIR light. However, there are two distinct regimes: optically thick to UV but thin to the re-radiated FIR and optically thick to FIR. We call these the “single-scattering” and “optically thick” limits, respectively.

2.1.1. Single-scattering Limit

Regions in the single-scattering limit are optically thick to the UV but optically thin to the FIR ($\tau_{\text{FIR}} \sim \kappa_{\text{FIR}}\Sigma_{\text{g}}/2$). This limit applies over a wide range in surface density:

$$\Sigma_{\text{g}} \lesssim 5000 \text{ M}_{\odot} \text{ pc}^{-2} \kappa_2^{-1} f_{\text{dg},150}^{-1}, \quad (3)$$

where $\kappa_{\text{FIR}} = \kappa_2 f_{\text{dg},150}$ is the Rosseland-mean dust opacity with $\kappa_2 = \kappa/(2 \text{ cm}^2 \text{ g}^{-1})$ (see §2.1.2) and $f_{\text{dg},150} = f_{\text{dg}} \times 150$ is

the dust-to-gas ratio. In the single-scattering limit, UV photons are absorbed once and then re-radiated as FIR photons, which free-stream out of the medium.⁵ Since the column-averaged flux-mean optical depth in this limit is always equal to unity, the flux-mean opacity for the single-scattering limit is $\sim 2/\Sigma_{\text{g}}$. The Eddington flux is then

$$F_{\text{Edd}}^{\text{s}} \sim 10^8 \text{ L}_{\odot} \text{ kpc}^{-2} \left(\frac{\Sigma_{\text{g}}}{10 \text{ M}_{\odot} \text{ pc}^{-2}} \right)^2 f_{\text{gas}}^{-1}, \quad (4)$$

where $f_{\text{gas}} = \Sigma_{\text{g}}/\Sigma_{\text{tot}}$ is the gas fraction and $\Sigma_{\text{tot}} \equiv \Sigma_{\text{g}} + 0.1\Sigma_{\star}$ (Wong & Blitz 2002). The wide range of column densities over which this limit is applicable implies that the average medium of most star-forming galaxies, some starbursts, and the GMCs that constitute them is single-scattering.

2.1.2. Optically Thick Limit

Dense starbursts and GMCs can reach the high gas surface densities $\Sigma_{\text{g}} \gtrsim 5000 \text{ M}_{\odot} \text{ pc}^{-2} \kappa_2^{-1} f_{\text{dg},150}^{-1}$ necessary to become optically thick to FIR photons ($\tau_{\text{FIR}} \gtrsim 1$). In this case $P_{\text{rad}} \sim \tau_{\text{FIR}} F/c$, and κ_{FIR} depends on temperature (Bell & Lin 1994; Semenov et al. 2003). The functional form of κ_{FIR} naturally leads to two regimes: “warm” ($T < 200 \text{ K}$) and “hot” ($200 \text{ K} < T < T_{\text{sub}}$, where $T_{\text{sub}} \sim 1500 \text{ K}$ is the dust sublimation temperature). For typical numbers, the central temperature of a massive, compact star cluster is

$$T^4 \sim \tau T_{\text{eff}}^4 \sim \frac{\kappa_{\text{FIR}} \Sigma}{2} \frac{F}{\sigma_{\text{SB}}} \sim \frac{\kappa_{\text{FIR}} M_{\text{g}}}{8\pi R^2} \frac{M_{\star} \Psi}{4\pi R^2 \sigma_{\text{SB}}} \\ T \sim 290 \text{ K} \kappa_{10}^{1/4} \Psi_{3000}^{1/4} M_{\text{g},6}^{1/4} M_{\star,5}^{1/4} R_{\text{pc}}^{-1}, \quad (5)$$

where T_{eff} is the effective temperature, $\kappa_{10} = \kappa/(10 \text{ cm}^2 \text{ g}^{-1})$, $\Psi_{3000} = 3000 \text{ ergs s}^{-1} \text{ g}^{-1}$ is the light-to-mass ratio of a zero age main sequence stellar population, $M_{\text{g},6} = M_{\text{g}}/(10^6 \text{ M}_{\odot})$, and $M_{\star,5} = M_{\star}/(10^5 \text{ M}_{\odot})$.

Warm Starbursts — For $T < 200 \text{ K}$, the Rosseland mean opacity increases as $\kappa_{\text{FIR}}(T) \approx \kappa_0 T^2$, where $\kappa_0 \approx 2 \times 10^{-4} \text{ cm}^2 \text{ g}^{-1} \text{ K}^{-2} f_{\text{dg},150}$. In this case,

$$F_{\text{Edd}} \approx \left(\frac{3\pi Gc\sigma_{\text{SB}}}{\kappa_0^2 f_{\text{dg},150}^2 f_{\text{gas}}} \right)^{1/2} \sim 10^{13} \text{ L}_{\odot} \text{ kpc}^{-2} f_{\text{gas}}^{-1/2} f_{\text{dg},150}^{-1}. \quad (6)$$

Remarkably, the flux necessary to support the medium is independent of Σ (TQM).

Hot Starbursts — Intense, compact starbursts may have central temperatures greater than 200 K. The corresponding opacity is roughly constant with temperature: $\kappa_{\text{FIR}}(T) \approx 5\text{--}10 \text{ cm}^2 \text{ g}^{-1} f_{\text{dg},150}$ for temperatures $200 \text{ K} \lesssim T \lesssim T_{\text{sub}}$. For typical numbers,

$$F_{\text{Edd}}^{\text{thick}} \sim 10^{15} \text{ L}_{\odot} \text{ kpc}^{-2} \left(\frac{\Sigma_{\text{g}}}{10^6 \text{ M}_{\odot} \text{ pc}^{-2}} \right) f_{\text{gas}}^{-1/2} f_{\text{dg},150}^{-1}. \quad (7)$$

The high surface densities necessary to enter this regime may only be attained in the pc-scale star formation thought to attend the fueling of bright AGN (Sirko & Goodman 2003; TQM; Levin 2007).

⁵ Galaxies with surface densities less than $\sim 5 \text{ M}_{\odot} \text{ pc}^{-2}$ will be optically thin with respect to dust. Below this limit, the ionization of neutral hydrogen will become the dominant source of opacity. The large cross-section ($\sigma_{\text{HI}} \approx 6.3 \times 10^{-18} \text{ cm}^2$ per H atom) implies an incredibly small surface density ($\Sigma_{\text{g}} \gtrsim 10^{-3} \text{ M}_{\odot} \text{ pc}^{-2}$) is required for the medium to be optically thick to ionizing photons. These ionizing photons transfer momentum directly to the gas on the same order as the momentum transfer due to the single-scattering limit for dust. Thus, we encompass this limit and the single-scattering limit for dust under the same heading.

2.2. GMC Evolution & Intermittency

In order to gauge the importance of GMC evolution and intermittency, we adopt the simple picture presented by MQT that marginally stable ($Q \approx 1$) disks fragment into sub-units on the gas disk scale height (h) to form GMCs. An individual star cluster is born, reaches the critical Eddington luminosity threshold, and then expels the overlying gas. Importantly, the timescale for collapse and expansion of the GMC is the disk dynamical timescale, t_{dyn} , which can be much longer than the characteristic timescale for the stellar population to decrease in total luminosity, the main-sequence lifetime of massive stars, $t_{\text{MS}} \sim 4 \times 10^6$ yr. In this picture, a low-density star-forming galaxy with radius r should have $\sim (r/h)^2$ sub-units, but only a small fraction ξ (the ‘‘intermittency factor’’) should be bright at any one time. If each subregion reaches the Eddington luminosity for a time t_{MS} and is then dark, and then if a large number of subregions are averaged, one expects

$$\xi \equiv \frac{N_{\text{on}}}{N_{\text{tot}}} \sim \frac{L_{\text{obs}}}{L_{\text{Edd}}} \sim \frac{t_{\text{MS}}}{2t_{\text{dyn}} + t_{\text{MS}}}, \quad (8)$$

where

$$t_{\text{dyn}} \sim \left(\frac{3\pi(2h)}{32G\Sigma_{\text{tot}}} \right)^{1/2} \\ \sim 3.5 \times 10^7 \text{ yr } h_{100}^{1/2} f_{\text{gas}}^{1/2} \left(\frac{10 M_{\odot} \text{ pc}^{-2}}{\Sigma_{\text{g}}} \right)^{1/2}, \quad (9)$$

$h_{100} = h/(100 \text{ pc})$, N_{on} is the number of sub-units that are ‘‘on,’’ and N_{tot} is the total number of sub-units. For example, the normal star-forming galaxy M51 has a observed bolometric luminosity ($L_{\text{obs}} = 0.2L_{\text{Edd}}$) that is a factor of ~ 4 larger than its intermittency-corrected Eddington luminosity ($L_{\text{Edd}}^{\text{int}} = 0.05L_{\text{Edd}}$). Although the approximation that the stellar population is bright for a time t_{MS} and then dark is crude, the parameter ξ gives us a way to judge the importance of intermittency in normal star-forming galaxies.

Note that for higher densities, t_{dyn} decreases and $\xi \rightarrow 1$ at a critical surface density

$$\Sigma_{\text{crit}} \sim \frac{3\pi(2h)}{32G(0.5t_{\text{MS}})^2} \sim 3 \times 10^3 M_{\odot} \text{ pc}^{-2} h_{100}, \quad (10)$$

which corresponds with a critical midplane pressure $P_{\text{crit}} \sim 5 \times 10^{-8} \text{ ergs cm}^{-3} h_{100}^2$ (see eq. 15). For $\Sigma_{\text{tot}} > \Sigma_{\text{crit}}$, massive stars live longer than the time required to disrupt the parent sub-unit ($t_{\text{MS}} > t_{\text{dyn}}$). MQT argue that in this regime the massive stars continue to drive turbulence in the gas and maintain hydrostatic equilibrium in a statistical sense until t_{MS} , when the process then repeats until gas exhaustion.

Several additional elements of GMC evolution are important in judging whether or not the star formation of galaxies is regulated by radiation pressure on dust. First, the GMCs collapse from regions of size h^2 , with total mass $\Sigma_{\text{g}}\pi h^2$, and to a size $R_{\text{GMC}} = h/\phi$. This implies that the surface density of individual GMCs is $\Sigma_{\text{GMC}} \sim \phi^2 \Sigma_{\text{g}}$, where ϕ can be ~ 2 – 5 in the Galaxy (MQT). For example, taking $\epsilon_{\text{GMC}} = M_{\star}/M_{\text{GMC}}$ ($\propto \Sigma_{\text{g}}$ in the single-scattering limit), Ψ_{3000} , and assuming $\kappa_{\text{FIR}} \sim \kappa_{\text{o}} T^2$ (appropriate for $T \lesssim 200 \text{ K}$), one finds that the required gas surface density for a GMC to be optically thick to the FIR is $\Sigma_{\text{GMC}}^{\tau_{\text{FIR}}=1} \sim 7000 \epsilon_{\text{GMC},0.1}^{-1/3} M_{\odot} \text{ pc}^{-2}$. This GMC gas surface density would correspond to an average gas surface density for the galaxy that is ϕ^2 times smaller ($\Sigma_{\text{g}} \sim 350$ – $1800 M_{\odot} \text{ pc}^{-2}$). Thus, the medium surrounding the central

star cluster may be optically thick to the FIR even if the average gas surface density of the galaxy is less than the naive estimate given in §2.1.2.

At surface densities in excess of $\tau_{\text{FIR}} = 1$ for the GMCs, the models of MQT rely on the fact that the medium is in fact optically-thick to FIR radiation. This is in sharp contrast to the work of KM09, where they argue that the effective optical depth is always ~ 1 because instabilities allow the radiation to leak out of otherwise optically-thick media. MQT argue that the effective optical depth must be much larger than unity in the GMCs of dense starbursts and ULIRGs for radiation pressure to be effective as a feedback mechanism. In addition, they show that the effective momentum coupling between the radiation and the gas can exceed the naive estimate based on a disk-averaged τ_{FIR} by a factor of a few in systems as dense as the putative GMCs in Arp 220 because of the time-dependence of the GMC disruption process (see §4.3).

3. RESULTS

We compile data of super star clusters, normal star-forming galaxies, local starburst galaxies, ULIRGs, sub-millimeter galaxies (SMGs), hyper luminous infrared galaxies, and circumnuclear starbursts to assess feedback from radiation pressure. Below, we test the hypothesis that radiation pressure is dynamically important in galaxies and star-forming subregions by comparing data to the Eddington limit (§2) on a variety of physical scales ranging from globally-averaged properties of galaxies to individual star-forming subregions within galaxies.

3.1. IR Luminosity vs. Molecular Line Luminosity

We show the total IR luminosity L_{IR} as a function of molecular line luminosity⁶ L'_{CO} (Figure 1) and L'_{HCN} (Figure 2) for our sample of star-forming galaxies.⁷ L_{IR} is known to trace the total light from massive stars (e.g., Kennicutt 1998),⁸ whereas L'_{CO} and L'_{HCN} provide a measure of the total gas mass and dense gas mass, respectively. Under the assumption that the total gravitational potential is dominated by the gas on the physical scales where the stars are forming, the Eddington luminosity is related to L'_{CO} by

$$L_{\text{Edd}} = \frac{4\pi Gc}{\kappa} X_{\text{CO}} L'_{\text{CO}}, \quad (11)$$

where X_{CO} is the L'_{CO} -to- M_{H_2} conversion factor and κ is the appropriate flux-mean or Rosseland-mean opacity (either

⁶ We used the $J = 1$ – 0 line unless only higher order lines were available.

⁷ Aravena et al. 2008; Becklin et al. 1980; Beelen et al. 2006; Benford et al. 1999; Capak et al. 2008; Carilli et al. 2005; Casoli et al. 1989; Chapman et al. 2005; Chung et al. 2009; Combes et al. 2010; Coppin et al. 2009; Coppin et al. 2010; Daddi et al. 2007; Daddi et al. 2009; Daddi et al. 2010a; Downes & Solomon 1998; Gao et al. 2007; Gao & Solomon 1999; Gao & Solomon 2004a,b; Genzel et al. 2003; Graciá-Carpio et al. 2008; Greve et al. 2005; Greve et al. 2006; Isaak et al. 2004; Kim & Sanders 1998; Knudsen et al. 2007; Mauersberger et al. 1996; Mirabel et al. 1990; Momjian et al. 2007; Murphy et al. 2001; Neri et al. 2003; Riechers et al. 2006; Riechers et al. 2007; Riechers et al. 2008; Sajina et al. 2008; Sakamoto et al. 2008; Sanders et al. 1991; Schinnerer et al. 2006; Schinnerer et al. 2007; Schinnerer et al. 2008; Smith & Harvey 1996; Solomon et al. 1997; Solomon & Vanden Bout 2005; Walter et al. 2003; Walter et al. 2009; Weiß et al. 2001; Yan et al. 2010; Young & Scoville 1982; Yun et al. 2001.

⁸ In reality, for normal galaxies a fraction of the UV and optical light escapes before being reprocessed by dust, and a fraction of the IR is diffuse and likely not associated with star formation (e.g., Kennicutt et al. 2010; Calzetti et al. 2010). The UV and IR luminosities are roughly equal at a bolometric luminosity of $L_{\text{bol}} \sim 10^{10} L_{\odot}$, but the UV luminosity is an order of magnitude larger than the IR luminosity at $L_{\text{bol}} \sim 10^{8.5} L_{\odot}$ (Martin et al. 2005). Thus, we expect that galaxies with $L_{\text{IR}} \lesssim 10^{10} L_{\odot}$ to move closer to the Eddington limit in Figure 1.

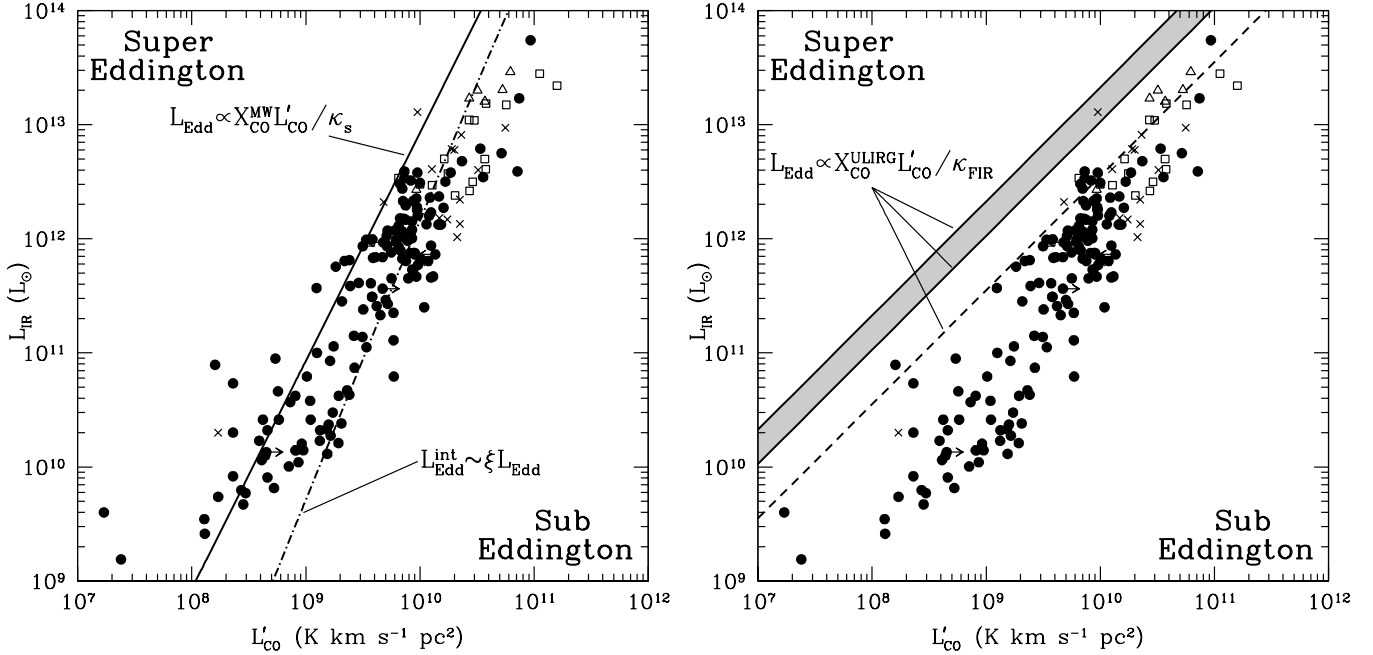


FIG. 1.— IR luminosity as a function of CO line luminosity. The different symbols correspond to different rotational transitions of CO: solid circles ($J = 1-0$), crosses ($J = 2-1$), squares ($J = 3-2$), and triangles ($J = 4-3$). The data are the same in both panels. The lines in the left panel correspond to the single-scattering Eddington limit (solid line; assuming $h = 100$ pc and $r = 10$ kpc; §2.1.1) and the single-scattering Eddington limit accounting for intermittency (dot-dashed line; eq. 8). The lines in the right panel show the optically thick Eddington limit for our preferred value of the Rosseland-mean opacity (shaded region; $\kappa_{\text{FIR}} = 5-10 \text{ cm}^2 \text{ g}^{-1} f_{\text{dg},150}$) and for an enhanced dust-to-gas ratio (dashed line; $\kappa_{\text{FIR}} = 30 \text{ cm}^2 \text{ g}^{-1} f_{\text{dg},50}$). Note that no galaxies are significantly super- or sub-Eddington. We emphasize that it is not possible to determine which limit is applicable without knowing a surface density, so dense star-forming regions can be optically thick at $L'_{\text{CO}} \lesssim 10^9 \text{ K km s}^{-1} \text{ pc}^2$ and approach the optically thick Eddington limit (see §2.1). The single-scattering Eddington limit was calculated by adopting the Galactic CO-to- H_2 conversion factor $X_{\text{CO}}^{\text{MW}} = 4.4 \text{ M}_{\odot} (\text{K km s}^{-1} \text{ pc}^2)^{-1}$. The optically thick Eddington limit was calculated by adopting the ULIRG CO-to- H_2 conversion factor $X_{\text{CO}}^{\text{ULIRG}} = 0.8 \text{ M}_{\odot} (\text{K km s}^{-1} \text{ pc}^2)^{-1}$.

single-scattering or optically thick; see §2.1.1–2.1.2). Although counterintuitive, the single-scattering Eddington luminosity lies below the optically thick Eddington limit because the dust opacity is column-averaged and highly non-grey (see §2.1). We adopt $X_{\text{CO}}^{\text{MW}} = 4.4 \text{ M}_{\odot} (\text{K km s}^{-1} \text{ pc}^2)^{-1}$ for normal galaxies (including a correction factor of 1.36 to account for He; Strong & Mattox 1996; Dame et al. 2001), and $X_{\text{CO}}^{\text{ULIRG}} = 0.8 \text{ M}_{\odot} (\text{K km s}^{-1} \text{ pc}^2)^{-1}$ for galaxies with $L_{\text{IR}} \geq 10^{11} L_{\odot}$ (as appropriate for starbursts and ULIRGs; e.g., Downes & Solomon 1998). Similarly, if the majority of the IR luminosity comes from regions where the dense molecular gas dominates the potential, then L_{Edd} is related to L'_{HCN} by

$$L_{\text{Edd}} = \frac{4\pi Gc}{\kappa_{\text{FIR}}} X_{\text{HCN}} L'_{\text{HCN}}, \quad (12)$$

where we explicitly write $\kappa = \kappa_{\text{FIR}}$ because the critical density for HCN emitting gas is large enough that these regions should always be optically-thick (§2.1.2).⁹ In eq. 12, we take an L'_{HCN} -to- $M_{\text{H}_2}^{\text{dense}}$ conversion factor of $X_{\text{HCN}} = 3 \text{ M}_{\odot} (\text{K km s}^{-1} \text{ pc}^2)^{-1}$, but we caution that X_{HCN} is uncertain to a factor of ~ 3 (Gao & Solomon 2004a,b; see §4.5).

In Figure 1, the lines indicate the Eddington limit for various limiting cases. The lines in the left panel show the single-scattering Eddington limit (solid line) and the single-scattering Eddington limit accounting for intermittency (dot-dashed line) assuming $h = 100$ pc and $r = 10$ kpc (eq. 11). The shaded region in the right panel is the optically thick Eddington limit (eq. 11 with $\kappa_{\text{FIR}} = 5-10 \text{ cm}^2 \text{ g}^{-1}$) and the dashed

line shows the optically thick Eddington limit for an enhanced opacity ($\kappa_{\text{FIR}} = 30 \text{ cm}^2 \text{ g}^{-1} f_{\text{dg},50}$; where $f_{\text{dg},50} = f_{\text{dg}} \times 50$) due to an assumed higher dust-to-gas ratio in dense star-forming environments. We plot the single-scattering (left panel) and optically thick (right panel) Eddington limits separately for clarity, but the data are the same in both panels. The different symbols indicate various rotational transitions of CO: solid circles ($J = 1-0$), crosses ($J = 2-1$), squares ($J = 3-2$), and triangles ($J = 4-3$).

Note that no galaxies exceed the optically thick Eddington limit and most galaxies are neither significantly super- or sub-Eddington with respect to the single-scattering Eddington limit. We caution that the applicable Eddington limit for any individual galaxy cannot be determined in this plot due to the lack of surface density measurements, which dictate the optical depth to the FIR and the relevant Eddington limit. For example, high surface density star-forming regions can be optically thick at $L'_{\text{CO}} \lesssim 10^9 \text{ K km s}^{-1} \text{ pc}^2$ and lie to the left of the single-scattering Eddington limit (solid line in left panel) but below the optically thick Eddington limit (shaded region in right panel). For the single-scattering limit, our assumption of $r = 10$ kpc is accurate to a factor of ~ 5 for most of the sample, but the single-scattering opacity scales as r^{-2} , so it is only accurate to a factor of ~ 25 . Some compact starbursts have radii much smaller than our assumed radius, so they are optically thick, even at low L'_{CO} and this explains why they exceed the single-scattering limit in the left panel but are below the optically thick limit in the right panel. In addition, note that the optically-thick Eddington limit is a hard upper bound to a galaxy's IR luminosity, which suggests that radiation pressure feedback may set the maximum SFR of a galaxy. In the

⁹ Using $\rho_{\text{crit,HCN}} \sim 10^{-19} \text{ g cm}^{-3}$, $\tau_{\text{FIR}} \sim \kappa_{\text{FIR}} \rho_{\text{crit,HCN}} R$ is larger than unity for scales $R \gtrsim \text{pc}$ and $\kappa_{\text{FIR}} \gtrsim \text{few cm}^2 \text{ g}^{-1}$.

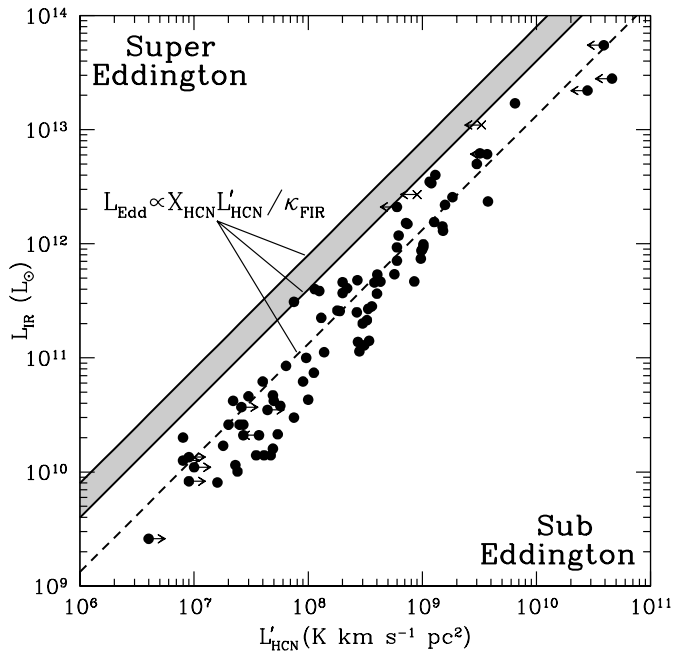


FIG. 2.— IR luminosity as a function of HCN line luminosity. The different symbols correspond to different rotational transitions of HCN: solid circles ($J = 1-0$) and crosses ($J = 2-1$). We show the optically thick Eddington limit for our preferred value of the Rosseland-mean opacity (shaded region; $\kappa_{\text{FIR}} = 5-10 \text{ cm}^2 \text{ g}^{-1} f_{\text{dg},150}$). The dashed line shows the effect of a factor of 3 increase in the dust-to-gas ratio for the optically thick Eddington limit ($\kappa_{\text{FIR}} = 30 \text{ cm}^2 \text{ g}^{-1} f_{\text{dg},50}$). Note that all galaxies are within ~ 1 dex of the optically thick Eddington limit, which suggests that radiation pressure may regulate star formation. The optically thick Eddington limit was calculated by adopting the HCN-to- H_2 conversion factor $X_{\text{HCN}} = 3 M_{\odot} (\text{K km s}^{-1} \text{ pc}^2)^{-1}$.

Eddington-limited model, the scatter in the $L_{\text{IR}}-L'_{\text{CO}}$ relation may be due to variations in h , X_{CO} (see §4.5), the dust-to-gas ratio/metallicity (see §4.4), the effective radii, and the depth of the stellar potential.¹⁰

The intermittency of star formation will likely affect the Eddington limit for CO-emitting gas (dot-dashed line in left panel). L'_{CO} traces the total molecular gas reservoir including the molecular gas that is not actively participating in star formation, such as GMC envelopes and diffuse intercloud gas. The gas mass relevant for the Eddington limit may be overestimated for galaxies in the single-scattering limit. To account for this, we multiply the Eddington luminosity by the intermittency factor for CO-emitting gas $\xi \sim 0.06$ for the Milky Way value of X_{CO} , $h = 100 \text{ pc}$, $r = 10 \text{ kpc}$, and $L'_{\text{CO}} = 10^9 \text{ K km s}^{-1} \text{ pc}^2$ (see eq. 8 and §2.2). The intermittency factor approaches unity when $L'_{\text{CO}} \sim 2 \times 10^{11} \text{ K km s}^{-1} \text{ pc}^2 h_{100} r_{10}^2 / X_{\text{CO}}^{\text{MW}}$. Thus, compact star-forming regions, such as the nuclear starbursts of ULIRGs, have $\xi \sim 1$ at low L'_{CO} due to their very small radii (e.g., Downes & Solomon 1998).

Figure 2 shows the $L_{\text{IR}}-L'_{\text{HCN}}$ relation for our sample of star-forming galaxies. The shaded region represents the optically-thick Eddington limit (eq. 12 with $\kappa_{\text{FIR}} = 5-10 \text{ cm}^2 \text{ g}^{-1}$) and the dashed line shows the optically thick Eddington limit for an enhanced opacity ($\kappa_{\text{FIR}} = 30 \text{ cm}^2 \text{ g}^{-1} f_{\text{dg},50}$; where $f_{\text{dg},50} = f_{\text{dg}} \times 50$), which may result from a higher dust-to-gas ratio

¹⁰ Note that previous work by Krumholz & Thompson (2007) and Narayanan et al. (2008) explains the slopes of the $L_{\text{IR}}-L'_{\text{CO}}$ and $L_{\text{IR}}-L'_{\text{HCN}}$ relations by comparing the critical density of the gas tracer to the median density of the ISM.

in dense star-forming environments. The circles and crosses correspond to the $J = 1-0$ and the $J = 2-1$ rotational transitions of HCN, respectively.

The $L_{\text{IR}}-L'_{\text{HCN}}$ relation (Figure 2) is tight and linear over several orders of magnitude, implying that stars form out of dense gas (Gao & Solomon 2004a,b; Wu et al. 2005). The dense gas fraction ($L'_{\text{HCN}}/L'_{\text{CO}}$) is nearly constant for galaxies with $L_{\text{IR}} \lesssim 10^{11} L_{\odot}$ (Gao & Solomon 2004b), so L'_{CO} can be used to indirectly trace the dense gas mass $M_{\text{H}_2}^{\text{dense}}$. However, the dense gas fraction increases dramatically in LIRGs and ULIRGs ($L_{\text{IR}} \gtrsim 10^{11} L_{\odot}$), so CO does not trace dense gas mass in these galaxies (Gao & Solomon 2004b). HCN, on the other hand, has a critical density for excitation that is ~ 2 orders of magnitude larger than that of CO, so it traces dense, optically thick gas in star-forming GMC cores rather than diffuse GMC envelopes. The dynamical time for HCN-emitting gas is much less than the main-sequence lifetime of the most massive stars, so the intermittency factor for HCN-emitting gas will be approximately unity:

$$t_{\text{dyn}}^{\text{HCN}} \sim 2 \times 10^5 \text{ yr } \rho_{\text{crit,HCN}}^{-1/2} \ll t_{\text{MS}} \rightarrow \xi \approx 1, \quad (13)$$

where $\rho_{\text{crit,HCN}} \sim 10^{-19} \text{ g cm}^{-3}$.

If the picture of radiation pressure feedback is correct, then it should determine the $L_{\text{IR}}-L'_{\text{HCN}}$ correlation directly. In fact, both the Eddington limit and the data show a linear relation between L_{IR} and L'_{HCN} . The galaxies closely follow but do not exceed the Eddington limit for our preferred value of the Rosseland-mean opacity ($\kappa_{\text{FIR}} = 5-10 \text{ cm}^2 \text{ g}^{-1} f_{\text{dg},150}$). If the opacity is higher ($\kappa_{\text{FIR}} = 30 \text{ cm}^2 \text{ g}^{-1} f_{\text{dg},50}$), then many galaxies are consistent with Eddington and a number are super-Eddington. For any of the values of the opacity that we assume, the general agreement between L_{IR} and L'_{HCN} suggests that radiation pressure may play an important role in regulating star formation (Scoville et al. 2003). However, a number of important factors remain uncertain, which we discuss in §4.

3.2. Molecular Schmidt Law and Radiation Pressure

The Schmidt law is a tight power law relation between the surface density of star formation rate $\dot{\Sigma}_{\star}$ and the gas surface density ($\dot{\Sigma}_{\star} \propto \Sigma_{\text{g}}^{1.4}$; Kennicutt 1998). Furthermore, Bigiel et al. (2008) found that the Schmidt law for molecular gas is linear within local star-forming galaxies ($\dot{\Sigma}_{\star} \propto \Sigma_{\text{H}_2}^{1.0}$). In the left panel of Figure 3, we plot $\dot{\Sigma}_{\star}$ vs. Σ_{H_2} for individual apertures of THINGS galaxies (small dots; Bigiel et al. 2008; Leroy et al. 2008), THINGS galaxies with H_2 detections (open circles), starburst galaxies¹¹ (solid circles), M82 super star clusters (stars; McCrady et al. 2003; McCrady & Graham 2007), and the Galactic Center star cluster (diamond; Paumard et al. 2006). We compare the data with the Eddington limit using $\dot{\Sigma}_{\star}$ and Σ_{H_2} as proxies for the radiation and gravitational forces,

$$\dot{\Sigma}_{\star}^{\text{Edd}} = \frac{4\pi G \Sigma_{\text{H}_2}}{\epsilon c \kappa}, \quad (14)$$

¹¹ Aravena et al. 2008; Becklin et al. 1980; Benford et al. 1999; Capak et al. 2008; Casoli et al. 1989; Chapman et al. 2005; Coppin et al. 2009; Coppin et al. 2010; Daddi et al. 2009; Downes & Eckart 2007; Downes & Solomon 1998; Greve et al. 2005; Knudsen et al. 2007; Mauersberger et al. 1996; Momjian et al. 2007; Neri et al. 2003; Paumard et al. 2006; Riechers et al. 2007; Riechers et al. 2008; Sajina et al. 2008; Sakamoto et al. 2008; Schinnerer et al. 2006; Schinnerer et al. 2007; Schinnerer et al. 2008; Smith & Harvey 1996; Walter et al. 2003; Walter et al. 2009; Weiß et al. 2001; Yan et al. 2010; Young & Scoville 1982; Yun et al. 2001

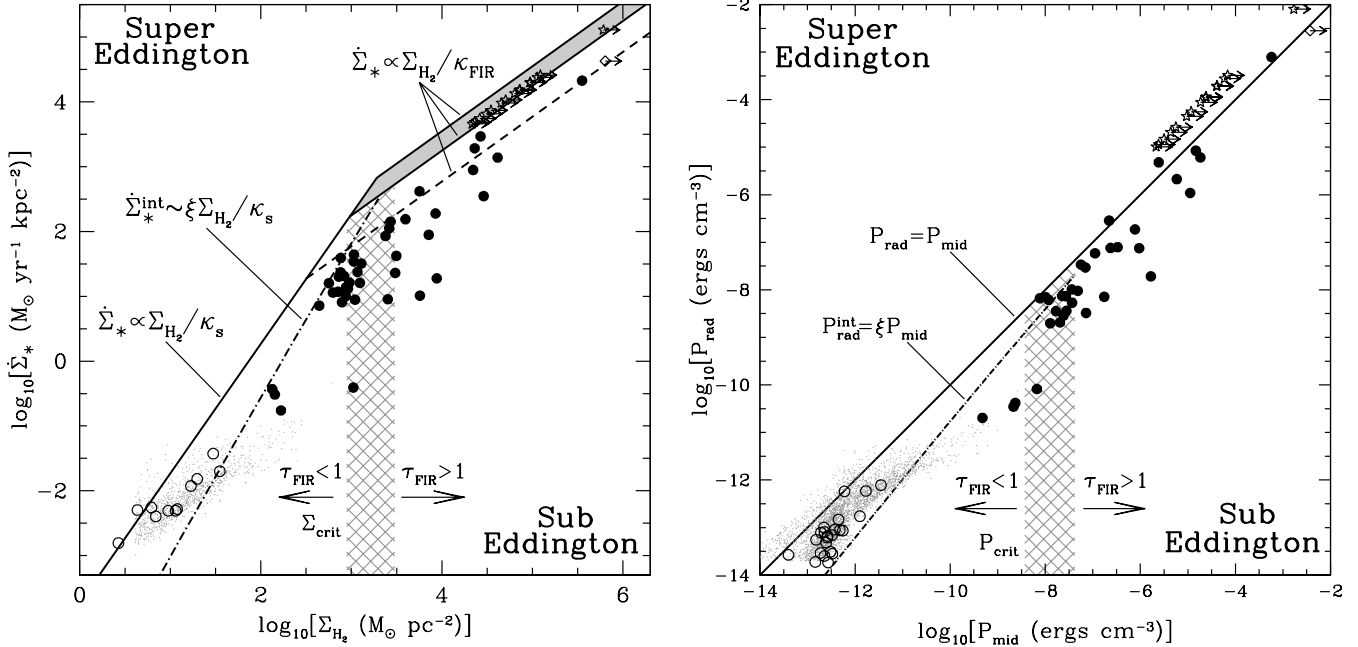


FIG. 3.— Star formation rate surface density ($\dot{\Sigma}_*$) as a function of the molecular gas surface density (Σ_{H_2}) (left panel) and radiation pressure as a function of midplane pressure (P_{mid} ; eq. 15) (right panel). The different symbols represent 750 pc apertures of THINGS galaxies (small dots), THINGS galaxies (open circles), starburst galaxies (solid circles), M82 super star clusters (stars), and the Galactic Center star cluster (diamond). The solid line in the $\dot{\Sigma}_*$ - Σ_{H_2} plot is the Eddington limit for the single-scattering ($\kappa = \kappa_s$) limit. The shaded region corresponds to the optically thick Eddington limit for our preferred value of the Rosseland-mean opacity ($\kappa_{\text{FIR}} = 5\text{--}10 \text{ cm}^2 \text{ g}^{-1} f_{\text{dg},150}$). The dashed line shows the effect of a factor of 3 increase in the dust-to-gas ratio for the optically thick Eddington limit ($\kappa_{\text{FIR}} = 30 \text{ cm}^2 \text{ g}^{-1} f_{\text{dg},50}$). In the $P_{\text{rad}}\text{--}P_{\text{mid}}$ plot, the solid line shows the Eddington limit adopting $\kappa_{\text{FIR}} = 10 \text{ cm}^2 \text{ g}^{-1} f_{\text{dg},150}$ for optically thick gas. The dot-dashed lines (both panels) are the intermittent Eddington limit (eq. 8). The hatched regions (both panels) are the critical surface density or pressure for $h = 30\text{--}100$ pc (eq. 10) where $t_{\text{MS}} \sim 2t_{\text{dyn}}$ and $\tau_{\text{FIR}} \sim 1$. Σ_{H_2} was calculated from L'_{CO} using $X_{\text{CO}}^{\text{MW}}$ if $L_{\text{IR}} < 10^{11} L_\odot$ and $X_{\text{CO}}^{\text{ULIRG}}$ if $L_{\text{IR}} > 10^{11} L_\odot$. Overall, the Eddington limit suggests that radiation pressure sets an upper bound to the $\dot{\Sigma}_*$ or the radiation pressure of a star-forming region or galaxy. Most star-forming regions or galaxies are sub-Eddington, but a few THINGS apertures and optically thick starbursts are super-Eddington (for $\kappa = 10 \text{ cm}^2 \text{ g}^{-1} f_{\text{dg},150}$). Several more optically thick starbursts will be consistent with or even exceed the Eddington limit for $\kappa = 30 \text{ cm}^2 \text{ g}^{-1} f_{\text{dg},50}$. The rough agreement between starburst galaxies and the intermittent Eddington limit reinforces the likely importance of intermittency. However, the intermittent Eddington limit mildly under-predicts $\dot{\Sigma}_*$ and P_{rad} at for $\Sigma_{\text{H}_2} \lesssim 10 \text{ M}_\odot \text{ pc}^{-2}$ and $P_{\text{mid}} \lesssim 10^{-12} \text{ ergs cm}^{-3}$, indicating that the effect of intermittency may be overestimated.

where $\epsilon \approx 5 \times 10^{-4}$ is the efficiency of the conversion of mass into luminosity during the star formation process assuming a Kroupa (2001) broken power law IMF that extends up to 120 M_\odot . For star clusters we assume a light-to-mass ratio appropriate for a zero age main sequence stellar population ($\Psi = 3000 \text{ ergs s}^{-1} \text{ g}^{-1}$) and that the stellar mass is a lower limit on the gas mass of the parent GMC. We use the same X_{CO} values as in Figure 1 and again caution that X_{CO} is uncertain to a factor of a few and may vary systematically from normal galaxies to starbursts (see §4.5).

For the molecular Schmidt law, we find that the Eddington limit is an upper bound to $\dot{\Sigma}_*$. Most star-forming regions and galaxies follow the Eddington limit (solid line) and are within ~ 1.5 dex of it. The Eddington limit accounting for intermittency (dot-dashed line) appears to agree better with the data than the naive single-scattering Eddington limit, suggesting that intermittency may be an important effect. As the medium becomes optically thick near the critical surface density for intermittency (hatched region; see §2.2), the optically thick Eddington limit ($\dot{\Sigma}_*^{\text{Edd}} \propto \Sigma_{\text{H}_2} / \kappa_{\text{FIR}} \propto \Sigma_{\text{H}_2}^{1.0}$) provides a firm upper bound to $\dot{\Sigma}_*$ for our preferred value of the dust opacity ($\kappa_{\text{FIR}} = 5\text{--}10 \text{ cm}^2 \text{ g}^{-1} f_{\text{dg},150}$). If the dust opacity ($\kappa_{\text{FIR}} = 30 \text{ cm}^2 \text{ g}^{-1} f_{\text{dg},50}$) is enhanced due to a higher assumed dust-to-gas ratio, then some galaxies reach the optically thick Eddington limit and a few galaxies exceed it.

In the right panel of Figure 3, we plot the radiation pres-

sure from UV and FIR photons versus the midplane pressure. These pressures will balance each other at Eddington (solid line):

$$P_{\text{rad}} \sim (1 + \tau_{\text{FIR}}) \frac{F}{c} \sim P_{\text{mid}} = \frac{\pi}{2} G \Sigma_{\text{g}} \Sigma_{\text{tot}}, \quad (15)$$

where we take $\Sigma_{\text{tot}} \equiv \Sigma_{\text{g}} + 0.1 \Sigma_*$ (Wong & Blitz 2002). The $P_{\text{rad}}\text{--}P_{\text{mid}}$ plot shows that radiation pressure correlates strongly with midplane pressure over 10 orders of magnitude. The Eddington limit serves as a rough upper limit to P_{rad} , and most galaxies are within 2 dex of the Eddington limit. We note that some of the THINGS apertures and some dense starbursts reach or exceed the Eddington limit. For galaxies with $P_{\text{mid}} < P_{\text{crit}}$, the critical midplane pressure (hatched region; see §2.2 & 4.2), we expect that the effects of intermittency are important; however, the intermittency adjusted Eddington limit (dot-dashed line) under-predicts P_{rad} for star-forming regions with $P_{\text{mid}} \lesssim 10^{-11.5} \text{ ergs cm}^{-3}$. The intermittency factor may overestimate the importance of intermittency because of the simplifying assumption that subregions are “on” or “off” (see §2.2). We also see that galaxies and star-forming regions with $10^{-11} \text{ ergs cm}^{-3} \lesssim P_{\text{mid}} \lesssim P_{\text{crit}}$ tend to fall significantly below the Eddington limit, possibly because our simple parametrization of X_{CO} (see §4.5) is overestimating M_{H_2} (and P_{mid}) for these systems. Radiation pressure becomes increasingly more important in the optically thick limit ($P_{\text{rad}} \gtrsim P_{\text{crit}}$) as some galaxies and star-forming regions meet and exceed Eddington. As expected from Figures 1 & 2, if we assume

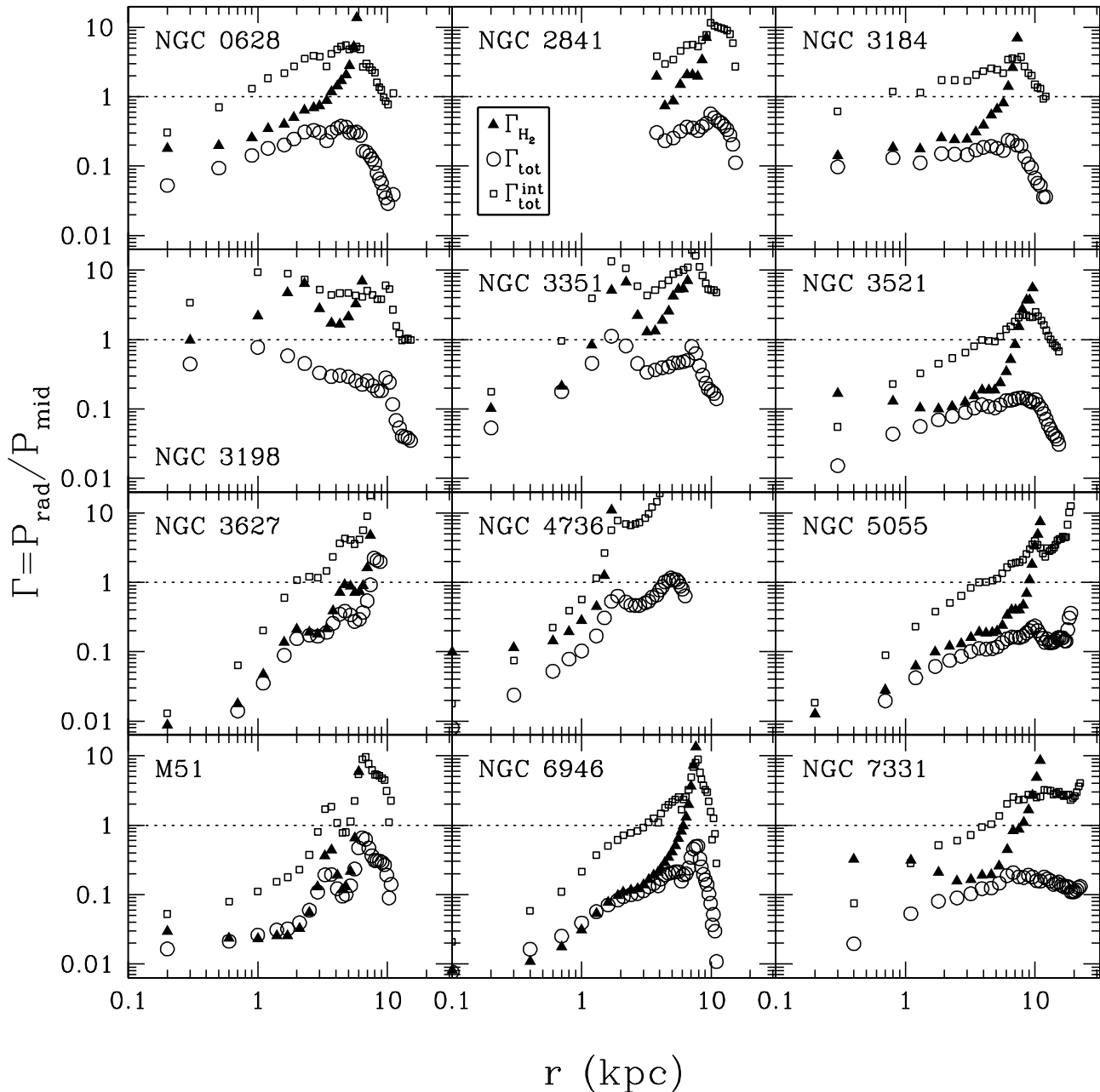


FIG. 4.— The Eddington ratio ($\Gamma = P_{\text{rad}}/P_{\text{mid}}$) as a function of radius for THINGS galaxies with H_2 detections. Γ_{H_2} ($= P_{\text{rad}}/(\pi G \Sigma_{\text{H}_2}^2)$; solid triangles) and Γ_{tot} ($= P_{\text{rad}}/(0.5\pi G \Sigma_{\text{g}} \Sigma_{\text{tot}})$; open circles) represent two ways to calculate the midplane pressure. The open squares ($\Gamma_{\text{tot}}^{\text{int}}$) show the effect of adjusting Γ_{tot} for intermittency (see eq. 8). Γ_{tot} tends to be sub-Eddington, rising to a peak at $r \sim 5\text{--}10$ kpc, and then rapidly falling off. However, $\Gamma_{\text{tot}}^{\text{int}}$ is super-Eddington for $r \gtrsim 1$ kpc in most of the galaxies, suggesting that ξ likely overestimates the importance of intermittency. Γ_{H_2} generally follows the trend of Γ_{tot} in the inner regions of galaxies but increases to super-Eddington values as Σ_{H_2} nears the detection threshold.

a larger dust-to-gas ratio and opacity ($\kappa = 30 \text{ cm}^2 \text{ g}^{-1} f_{\text{dg},50}$) potentially appropriate for dusty galaxies, then more of the optically thick starbursts would be super-Eddington.

3.3. Radiation Pressure on Sub-galactic Scales

So far we have evaluated radiation pressure on a galaxy-wide scale; however, the distribution of gas and star formation in galaxies is inhomogeneous. Consequently, the Eddington ratio ($\Gamma = P_{\text{rad}}/P_{\text{mid}}$) will likely vary on sub-galactic scales. We use observations from the THINGS survey (Walter et al. 2008; Leroy et al. 2008; Bigiel et al. 2008) to calcu-

late the Eddington ratio as a function of radius in azimuthally averaged radial bins and for semi-resolved (750 pc) apertures. Since the THINGS galaxies are generally in the single-scattering limit (see eq. 3), we conservatively adopt the radiation pressure to be $P_{\text{rad}}^{\text{IR}} = F_{\text{IR}}/c$ (see eq. 15). For the midplane pressure given in eq. 15, the corresponding Eddington ratio is $\Gamma_{\text{tot}} = P_{\text{rad}}^{\text{IR}}/(0.5\pi G \Sigma_{\text{g}} \Sigma_{\text{tot}})$. Stars and atomic gas may not contribute significantly to the surface density in regions of active star formation, so we also calculate the Eddington ratio assuming that the midplane pressure depends only on the total gas surface density $\Gamma_{\text{g}} = P_{\text{rad}}^{\text{IR}}/(\pi G \Sigma_{\text{g}}^2)$ or the molecular gas

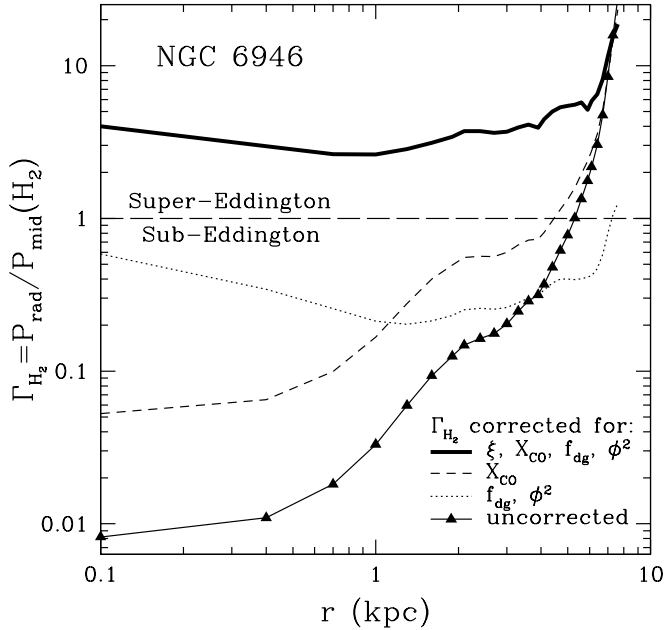


FIG. 5.— The molecular gas Eddington ratio $\Gamma_{\text{H}_2} = P_{\text{rad}}/(\pi G \Sigma_{\text{H}_2}^2)$ as a function of radius for NGC 6946. The line styles show the uncorrected Eddington ratio (triangles and thin solid line) and Γ_{H_2} corrected for an X_{CO} gradient (dashed line), for a dust-to-gas ratio gradient plus a factor of ϕ^2 ($\phi = h/R_{\text{GMC}}$; see §2.2; dotted line), and for X_{CO} and dust-to-gas ratio gradients plus the intermittency factor and the ϕ^2 factor (thick solid line). After all of these factors are accounted for, the Eddington ratio is ~ 1 and nearly flat as a function of radius. We only show the effects of the X_{CO} and dust-to-gas ratio gradients on the Eddington ratio in NGC 6946, but the profiles from the other THINGS galaxies shown in Figure 4 are qualitatively similar.

surface density $\Gamma_{\text{H}_2} = P_{\text{rad}}^{\text{IR}}/(\pi G \Sigma_{\text{H}_2}^2)$. Intermittency may be important because the THINGS observations cannot resolve individual star-forming regions. We calculate the Eddington ratio corrected for intermittency ($\Gamma_{\text{tot}}^{\text{int}} = \Gamma_{\text{tot}}/\xi$, see eq. 8). In Figure 4, we plot Γ_{tot} (open circles), Γ_{H_2} (solid triangles), and $\Gamma_{\text{tot}}^{\text{int}}$ (open squares) as a function of radius for azimuthally averaged rings. We find that Γ_{g} is similar to Γ_{tot} , so we omit Γ_{g} for clarity.

At intermediate radii ($r \sim 1 \rightarrow$ several kpc), Γ_{tot} and Γ_{H_2} generally increase from sub-Eddington ($\Gamma \sim 0.1$) to approaching or exceeding the Eddington limit ($\Gamma \sim 1$). Γ_{tot} reaches a maximum Eddington ratio at $r \sim 5\text{--}10$ kpc, where it falls off steeply. As the observations near the H_2 detection threshold, Γ_{H_2} increases rapidly due to a small Σ_{H_2} with large error bars (see, e.g., Figure 40 from Leroy et al. 2008), and thus the large value of Γ_{H_2} at large r is consistent with Eddington to within the errors on Σ_{H_2} . For $r > 1$ kpc where $\Gamma_{\text{tot}} < 1$, the intermittency factor can boost $\Gamma_{\text{tot}}^{\text{int}}$ to the Eddington limit, suggesting that intermittency is important.

The $\Gamma < 1$ regions in the inner parts of star-forming galaxies present a challenge for radiation pressure regulated star formation. Intermittency cannot account for the low Eddington ratios of these regions. However, a metallicity gradient, as seen in observations of star-forming galaxies (Muñoz-Mateos et al. 2009), increases the Eddington ratio at small radii (see §4.4). A metallicity gradient that rises at smaller radii correlates with a decreasing gradient in X_{CO} (Sodroski et al. 1995; Arimoto et al. 1996) and an increasing gradient in the dust-to-gas ratio (Muñoz-Mateos et al. 2009). We adopt the X_{CO} gradient given by eq. 10 of Arimoto et al. (1996) for data from the

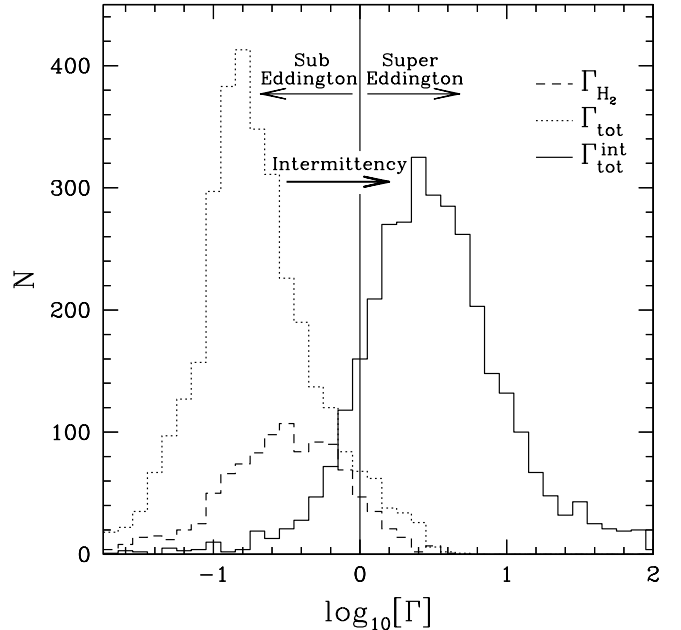


FIG. 6.— Histogram of the Eddington ratio ($\Gamma = P_{\text{rad}}/P_{\text{mid}}$) for 750 pc apertures of THINGS galaxies. The midplane pressure was calculated using two different methods: $\Gamma_{\text{H}_2} = P_{\text{rad}}/(\pi G \Sigma_{\text{H}_2}^2)$ (dashed line) and $\Gamma_{\text{tot}} = P_{\text{rad}}/(0.5\pi G \Sigma_{\text{g}} \Sigma_{\text{tot}})$ (dotted line). The solid line ($\Gamma_{\text{tot}}^{\text{int}}$) shows the effect of adjusting the Eddington ratio by the intermittency factor (eq. 8). Γ_{tot} was calculated for all apertures with either an H_2 or HI detection, but Γ_{H_2} could be calculated only for apertures with H_2 detections. The Γ_{tot} distribution is mostly sub-Eddington, but intermittency pushes the majority of the $\Gamma_{\text{tot}}^{\text{int}}$ distribution above the Eddington limit, implying that ξ may overestimate the importance of intermittency. The Γ_{H_2} distribution is less peaked and shifted to higher Eddington ratios than the Γ_{tot} distribution. Some apertures in the Γ_{H_2} distribution are at or above the Eddington limit in spite of the observations not being able to resolve individual star-forming regions.

Milky Way, M31, and M51 ($\log X/X_e = 0.41[r/r_e - 1]$, where r_e is the effective radius, which we assume to be 7 kpc and X_e is the value of X_{CO} at the effective radius). To account for the dust-to-gas ratio gradient, we use a power law interpolation between $f_{\text{dg}} = 1/30$ at 0.1 kpc and $f_{\text{dg}} = 1/150$ at 10 kpc, motivated by Figure 15 of Muñoz-Mateos et al. (2009). In addition, collapsing GMCs enhance the surface density by a factor of ϕ^2 ($\phi = h/R_{\text{GMC}}$; see 2.2), making some regions optically thick to FIR radiation. In Figure 5, we show the molecular Eddington ratio as a function of radius for NGC 6946 since this galaxy is well below (~ 2 dex) the Eddington limit at small radii (see Figure 4). After accounting for intermittency, an X_{CO} gradient, a dust-to-gas ratio gradient, and a surface density enhancement in the GMCs, we find that $\Gamma_{\text{H}_2} \sim 1$ for almost all radii in NGC 6946. We find qualitatively similar results for all of the THINGS galaxies shown in Figure 4 assuming that the metallicity, X_{CO} , and dust-to-gas ratio gradients are similar to those adopted for NGC 6946. Thus, it is at least in principle possible to explain the nominally sub-Eddington inner regions of local star-forming galaxies using a combination of these effects.

In Figure 6, we plot the distributions of the individual Eddington ratios for the THINGS apertures (750 pc resolution): Γ_{tot} (dotted line), Γ_{H_2} (dashed line), and $\Gamma_{\text{tot}}^{\text{int}}$ (solid line). The distribution of Γ_{tot} is peaked around $\Gamma_{\text{tot}} \sim 0.1$, and the majority of apertures are sub-Eddington for Γ_{tot} . The high Γ_{tot} tail of the distribution extends above the Eddington limit, with super-Eddington apertures comprising 5% of the total aper-

tures and containing 5% of the total flux. Star-forming regions are unresolved on 750 pc scales, so Γ_{tot} should be adjusted to account for intermittency ($\Gamma_{\text{tot}}^{\text{int}}$). However, most apertures lie above the intermittency adjusted Eddington limit. As in Figures 1–5, this shift suggests that intermittency is important for radiation pressure supported star formation in normal spirals; however, ξ appears to overestimate the importance of intermittency, possibly due to the simplifying assumption that subregions are either “on” or “off” (see §2.2 & 4.2). The distributions of Γ_{tot} and Γ_{g} are similar, so we do not plot Γ_{g} for clarity.

The distribution of Γ_{H_2} is less peaked and shifted to systematically higher values than the distribution of Γ_{tot} with 10% of these apertures radiating at or above the Eddington limit. This is not surprising (given Figure 4) because radiation pressure will likely be more important in H_2 -dominated star-forming regions. The detection limit for H_2 is higher than that for HI, so the distribution of Γ_{H_2} contains fewer apertures than Γ_{tot} . In addition, the apertures with H_2 detections tend to be within $0.4R_{25}$ (Bigiel et al. 2008), so they might have increased metallicities and dust-to-gas ratios with depressed X_{CO} values, which would increase the Eddington ratio (see Figure 5, §4.4 and 4.5). Super-Eddington apertures contain 6% of the total flux in H_2 -detected apertures across the whole sample; in NGC 6946, for example, super-Eddington apertures contain 10% of the total flux. The super-Eddington apertures indicate that radiation pressure can be dynamically dominant even when individual star-forming regions remain unresolved, suggesting that radiation pressure may be more important on the scale of GMCs and massive star clusters. Finally, we calculated Γ_{H_2} assuming that UV photons contribute to the radiation pressure $P_{\text{rad}} = (F_{\text{UV}} + F_{\text{IR}})/c$. The distribution of Γ_{H_2} remains nearly the same because star-forming regions have $F_{\text{IR}}/F_{\text{UV}} \gg 1$, so we refrain from plotting it in Figure 6.

4. DISCUSSION

We have compared globally-averaged and resolved observations of star-forming galaxies with theoretical expectations based on the theory of radiation pressure supported star formation (see §2). Although the uncertainties are large (see below), our primary findings are as follows.

1. Figures 1–3 show that star-forming galaxies meet, but do not dramatically exceed, nominal expectations for the dust Eddington limit. When some subregions do seem to exceed the Eddington limit (as in the outer regions of galaxies in Figure 4 & 5), we consider this to be consistent with Eddington since trends in the dust-to-gas ratio and CO-to- H_2 conversion factor, as well as the large-scale stellar potential and intermittency of the star-formation process (ξ ; eq. 8) affect the Eddington ratio at order unity.

2. The $L_{\text{IR}}-L'_{\text{HCN}}$ plot (Figure 2) provides the strongest evidence for the importance of radiation pressure feedback since L'_{HCN} is expected to directly trace the dense actively star-forming gas and L_{IR} traces the total star formation rate. If radiation pressure in fact dominates feedback, we would expect a one-to-one correspondence between these two quantities, and such a relation is observed (see also Scoville et al. 2001; Scoville 2003). Nevertheless, for typical values of both κ in the optically thick limit and the HCN-to- H_2 conversion factor, the Eddington limit overpredicts L_{IR} by a factor of $\sim 3-6$. This discrepancy may indicate that the dust-to-gas ratio is larger in the dense HCN-emitting regions,

or that the HCN-to- H_2 conversion factor is smaller (see §4.5 below). If radiation pressure feedback regulates star formation, then this relation is in a sense more fundamental than the Schmidt Law because HCN-emitting gas is more closely connected with star formation than CO-emitting gas, in which case we would expect $\Sigma_{\star}^{\text{Edd}} = 4\pi G \Sigma_{\text{H}_2}^{\text{dense}} / (\epsilon c \kappa_{\text{FIR}})$.

3. The central regions of all galaxies in Figure 4 are *prima facie* substantially sub-Eddington when a constant dust-to-gas ratio and CO-to- H_2 conversion factor are applied to all subregions without regard to their radial location. If radiation pressure is in fact the dominant feedback mechanism in these regions, a much higher central dust-to-gas ratio and a lower CO-to- H_2 conversion factor are required (see Figures 4 & 5). It would be particularly useful for testing radiation pressure feedback to produce the same profiles in HCN.

4. The “break” in the observed Schmidt Law at $\Sigma_{\text{g}} \sim 100-1000 M_{\odot} \text{ pc}^{-2}$ (see Figure 3; Daddi et al. 2010b) may be due to the transition from the single-scattering limit to the optically thick limit in the GMCs that collapse to form stars, as in MQT.

5. If radiation pressure is the primary feedback mechanism for regulating star formation, then we predict that the Schmidt Law will follow the form of eq. 14 (for discussion of κ and ξ as well as uncertainties see §2 & 4.2–4.5).

6. A testable prediction of radiation pressure feedback is that all else being equal the star formation rate should depend linearly on the dust-to-gas ratio in the optically thick limit.

In addition to these points, below we note an implication of radiation pressure feedback that has so far not been stated in the literature (§4.1). Finally, in the remaining subsections we highlight the dominant uncertainties in our work as a guide for future research on the importance of radiation pressure feedback in star-forming galaxies.

4.1. Gas Depletion Timescale

The gas depletion timescale, the time required to consume a galaxy’s gas reservoir at the current SFR, is observed to be ~ 2 Gyr in normal spirals (Kennicutt 1998; Leroy et al. 2008). Radiation pressure sets the gas depletion timescale to be

$$t_{\text{gas}} = \frac{M_{\text{g}}}{\dot{M}_{\star}} = \frac{M_{\text{g}} \epsilon c^2}{\xi L_{\text{Edd}}} = \frac{\epsilon c \kappa}{4\pi G \xi}. \quad (16)$$

Using typical numbers for a spiral galaxy in the single-scattering limit, the gas depletion timescale is

$$t_{\text{gas}} \sim 2.1 \text{ Gyr } \Sigma_{30}^{-3/2} h_{100}^{1/2}, \quad (17)$$

where $\Sigma_{30} = \Sigma/30 M_{\odot} \text{ pc}^{-2}$ and $h_{100} = h/100 \text{ pc}$. This normalization of t_{gas} is in good agreement with the observed gas depletion timescale, but eq. 17 predicts that the gas depletion timescale should have a strong dependence on Σ_{g} , in contrast to the observations of Leroy et al. (2008) (see their Figure 15). For completeness, we note that variations in the dust-to-gas ratio will not affect the dependence of t_{gas} on Σ_{g} in the single-scattering limit, but uncertainties in X_{CO} , ξ , and ϕ (see §4.4–4.5) might impact the gas depletion timescale.

Hot starbursts and optically thick subregions (see §2.1.2) have intermittency factors that approach unity and nearly constant opacities, so the gas depletion time is approximately

constant,

$$t_{\text{gas}} \approx 5.7 \text{ Myr } \kappa_{10}, \quad (18)$$

where $\kappa_{10} = \kappa_{\text{FIR}}/10 \text{ cm}^2 \text{ g}^{-1}$. For comparison, Sakamoto et al. (2008) find that the optically thick western nucleus of Arp 220 has a gas depletion time of ~ 6 Myr. The fact that the gas depletion timescale set by radiation pressure is consistent with the observed gas depletion timescale in spirals and ULIRGs is equivalent to the statement of Figures 1–5 that starbursts approach the dust Eddington limit. In addition, we point out that radiation pressure feedback predicts that the specific SFR (SSFR) will be $\text{SSFR} \sim 4\pi G \xi f_{\text{gas}} / (c \epsilon \kappa)$ for small f_{gas} .

4.2. Intermittency

The intermittency factor ξ (see §2.2; MQT) relates the properties of radiation pressure dominated star-forming subregions to the global properties of a galaxy. However, ξ may overestimate the effect of intermittency in some galaxies (see Figures 3, 4, & 6). We expect the determination of ξ to be complicated by uncertainty in the timescale for the central cluster of a sub-unit to be bright ($t_{\text{MS}} \sim 4$ Myr). We adopt t_{MS} as the time a cluster will be bright, since the cluster luminosity drops rapidly after the most massive stars in the cluster explode as supernovae. However, a cluster will continue to emit after t_{MS} . Indeed, models of cluster luminosity indicate that a similar amount of momentum will be transferred to the gas during the time $t_0 \rightarrow t_{\text{MS}}$ and during the time $t_{\text{MS}} \rightarrow 4t_{\text{MS}}$, where the cluster luminosity has dropped by 1 dex after $\sim 4t_{\text{MS}}$ (Leitherer et al. 1999). Further uncertainty in ξ is due to ambiguities in calculating the lifetime of a sub-unit ($\sim 2t_{\text{dyn}} + t_{\text{MS}}$), especially the disk dynamical time (see eq. 9). The dynamical time likely varies with galactocentric radius because Σ is a strong function of radius (Leroy et al. 2008). Thus, trying to determine an effective ξ applicable to a galaxy as a whole may be difficult if ξ changes locally. Overall, we expect the uncertainty in ξ to be a factor of a few to several.

4.3. The FIR Optical Depth

A key theoretical uncertainty in calculating the Eddington limit for dense starbursts is the effective optical depth (τ_{eff}) for surface densities where $\tau_{\text{FIR}} > 1$. In order for radiation pressure to be dynamically important in optically thick GMCs, τ_{eff} must exceed unity. Based on the high Mach number turbulence simulations of Ostriker et al. (2001), MQT conclude that if the ISM is optically thick on average, then the vast majority of sight lines will be optically thick. For comparison, KM09 argue that instabilities, such as Rayleigh-Taylor and photon-bubble instabilities, will reduce the effective optical depth of the dense ISM to ~ 1 . However, MQT note that both the midplane pressure from gravity $P_{\text{mid}} \sim \pi G \Sigma^2$ and optically thick radiation pressure $P_{\text{rad}} \sim \tau F / c \propto \Sigma^2$ scale as Σ^2 , a feature unique to radiation pressure among stellar feedback processes. Thus, if radiation pressure cannot regulate star formation in dense, optically thick gas, then no known stellar feedback process can.

4.4. Dust-to-Gas Ratio and Metallicity

The coupling between radiation and gas directly depends on the dust-to-gas ratio ($\kappa \propto f_{\text{dg}}$). In this analysis, we assume the Galactic value for the dust-to-gas ratio ($f_{\text{dg}} = 1/150$) and solar metallicity; however, there is strong evidence that f_{dg} and metallicity change with environment. The dust-to-gas ratio has been shown to correlate with metallicity and radius (Issa et al. 1990; Lisenfeld & Ferrara 1998; Draine

et al. 2007; Muñoz-Mateos et al. 2009). Muñoz-Mateos et al. (2009) find that the dust-to-gas ratio can climb to values as high as $f_{\text{dg}} \sim 1/10$ in the centers of spiral galaxies. This increase in metallicity and dust-to-gas ratio is necessary for the centers of star-forming spirals to be at Eddington (see Figures 4 & 5 and §3.3). The average dust-to-gas ratio of local spirals also varies by a factor of a few (e.g., M51 has a $f_{\text{dg}} \sim 1/75$; Draine et al. 2007). Furthermore, the dust-to-gas ratio is observed to be higher in some dense starbursts, such as SMGs ($f_{\text{dg}} \sim 1/50$; Kovács et al. 2006; Michałowski et al. 2010) and sub-mm faint ULIRGs ($f_{\text{dg}} \sim 1/20$; Casey et al. 2009). Importantly, if we adopt a dust-to-gas ratio potentially appropriate for dusty starbursts (short dashed line in Figure 1, 2, and the left panel of Figure 3), then a substantial fraction of optically thick galaxies would be at or above the Eddington limit (Figure 5 illustrates this for NGC 6946).

4.5. Molecular Gas Tracers

The Eddington limit depends strongly on the CO-to- H_2 (X_{CO}) and the HCN-to- H_2 (X_{HCN}) conversion factors (see eqs. 11 & 12). These conversion factors are two of the largest sources of observational uncertainty in our calculations because they vary with excitation conditions ($X \propto \sqrt{n_{\text{H}_2}}/T_{\text{b}}$, where T_{b} is the brightness temperature) and metallicity. Several lines of evidence suggest that $X_{\text{CO}}^{\text{MW}}$ overestimates M_{H_2} in starburst galaxies. For example, X_{CO} is a factor of ~ 3 lower in M82 (Weiss et al. 2001) and a factor of ~ 5 lower in a sample of local ULIRGs (Downes & Solomon 1998). To account for the different values of X_{CO} in normal spirals and extreme starbursts, we apply the Milky Way X_{CO} value to galaxies with $L_{\text{IR}} < 10^{11} L_{\odot}$ and the ULIRG X_{CO} value to galaxies with $L_{\text{IR}} > 10^{11} L_{\odot}$. Because this prescription is somewhat simplistic, it probably overestimates M_{H_2} in moderate luminosity starbursts ($L_{\text{IR}} < 10^{11} L_{\odot}$), such as M82, and in the centers of star-forming spirals (see Figures 4 & 5 and §3.3). Additionally, it likely underestimates M_{H_2} in ultra-luminous ($L_{\text{IR}} \sim 10^{12} L_{\odot}$) high redshift disk (BzK) galaxies, for which Daddi et al. (2010a) find a value of X_{CO} that is consistent with the Galactic value. As a result, moderate luminosity starbursts and the centers of star-forming spirals may be closer to Eddington and BzK galaxies might be further below the optically thick Eddington limit than Figure 3 would suggest.

Unfortunately, X_{HCN} is more uncertain than X_{CO} because there is no direct calibration of X_{HCN} from Milky Way GMCs. For normal spirals, Gao & Solomon (2004a,b) find $X_{\text{HCN}} \sim 10 M_{\odot} (\text{K km s}^{-1} \text{ pc}^2)^{-1}$ for virialized cloud cores with $\langle n \rangle = 3 \times 10^4 \text{ cm}^{-3}$ and $T_{\text{b}} = 35 \text{ K}$. They caution that X_{HCN} could be lower in regions of massive star formation due to significantly higher brightness temperatures $T_{\text{b}} \sim \text{few} \times 10^2 \text{ K}$ (Boonman et al. 2001). Ultra-luminous starbursts exhibit widespread intense massive star formation, so one might expect that X_{HCN} is lower in more luminous galaxies. For example, Graciá-Carpio et al. (2008) estimate that X_{HCN} should be ~ 4.5 times lower for galaxies at $L_{\text{FIR}} \sim 10^{12} L_{\odot}$ than at $L_{\text{FIR}} \sim 10^{11} L_{\odot}$. We note that if X_{HCN} is smaller than the assumed value of $3 M_{\odot} (\text{K km s}^{-1} \text{ pc}^2)^{-1}$, then more galaxies will approach or exceed the Eddington limit (see Figure 2). For example, decreasing X_{HCN} by a factor of ~ 2 brings essentially all galaxies in line with the Eddington limit for the nominal value of κ_{FIR} (~ 5 –10).

We thank N. Murray, E. Quataert, P. Hopkins, P. Martini, and R. Pogge for helpful conversations. We thank A. Leroy,

F. Bigiel, L. Yan, E. Daddi, T. Greve, and D. Riechers for providing us with their data. We also thank the referee, Mark Krumholz, for a timely and useful report, and for emphasizing

the point made in footnote 5. T.A.T. is supported in part by an Alfred P. Sloan Foundation Fellowship. This work is supported by NASA grant #NNX10AD01G.

REFERENCES

- Aravena, M., et al. 2008, *A&A*, 491, 173
 Arimoto, N., Sofue, Y., & Tsujimoto, T. 1996, *PASJ*, 48, 275
 Becklin, E. E., Gatley, I., Matthews, K., Neugebauer, G., Sellgren, K., Werner, M. W., & Wynn-Williams, C. G. 1980, *ApJ*, 236, 441
 Beelen, A., Cox, P., Benford, D. J., Dowell, C. D., Kovács, A., Bertoldi, F., Omont, A., & Carilli, C. L. 2006, *ApJ*, 642, 694
 Bell, K. R., & Lin, D. N. C. 1994, *ApJ*, 427, 987
 Benford, D. J., Cox, P., Omont, A., Phillips, T. G., & McMahon, R. G. 1999, *ApJ*, 518, L65
 Bigiel, F., Leroy, A., Walter, F., Brinks, E., de Blok, W. J. G., Madore, B., & Thornley, M. D. 2008, *AJ*, 136, 2846
 Blitz, L., Fukui, Y., Kawamura, A., Leroy, A., Mizuno, N., & Rosolowsky, E. 2007, *Protostars and Planets V*, 81
 Bolatto, A. D., Leroy, A. K., Rosolowsky, E., Walter, F., & Blitz, L. 2008, *ApJ*, 686, 948
 Boonman, A. M. S., Stark, R., van der Tak, F. F. S., van Dishoeck, E. F., van der Wal, P. B., Schäfer, F., de Lange, G., & Laauwen, W. M. 2001, *ApJ*, 553, L63
 Calzetti, D., et al. 2010, *ApJ*, 714, 1256
 Capak, P., et al. 2008, *ApJ*, 681, L53
 Carilli, C. L., et al. 2005, *ApJ*, 618, 586
 Casey, C. M., et al. 2009, *arXiv:0910.5756*
 Casoli, F., Combes, F., Augarde, R., Figon, P., & Martin, J. M. 1989, *A&A*, 224, 31
 Chapman, S. C., Blain, A. W., Smail, I., & Ivison, R. J. 2005, *ApJ*, 622, 772
 Chevalier, R. A., & Fransson, C. 1984, *ApJ*, 279, L43
 Chung, A., Narayanan, G., Yun, M. S., Heyer, M., & Erickson, N. R. 2009, *AJ*, 138, 858
 Combes, F., Garcia-Burillo, S., Braine, J., Schinnerer, E., Walter, F., & Colina, L. 2010, *arXiv:1009.2040*
 Coppin, K. E. K., et al. 2009, *MNRAS*, 395, 1905
 Coppin, K. E. K., et al. 2010, *MNRAS*, 407, L103
 Cunningham, A. J. 2008, Ph.D. Thesis,
 Daddi, E., et al. 2007, *ApJ*, 670, 156
 Daddi, E., et al. 2009, *ApJ*, 694, 1517
 Daddi, E., et al. 2010a, *ApJ*, 713, 686
 Daddi, E., et al. 2010b, *ApJ*, 714, L118
 Dame, T. M., Hartmann, D., & Thaddeus, P. 2001, *ApJ*, 547, 792
 Dickman, R. L., Snell, R. L., & Schloerb, F. P. 1986, *ApJ*, 309, 326
 Downes, D., & Eckart, A. 2007, *A&A*, 468, L57
 Downes, D., & Solomon, P. M. 1998, *ApJ*, 507, 615
 Draine, B. T. 2010, *arXiv:1003.0474*
 Draine, B. T., et al. 2007, *ApJ*, 663, 866
 Elmegreen, B. G. 1989, *ApJ*, 338, 178
 Ferrara, A. 1993, *ApJ*, 407, 157
 Gao, Y., Carilli, C. L., Solomon, P. M., & Vanden Bout, P. A. 2007, *ApJ*, 660, L93
 Gao, Y., & Solomon, P. M. 1999, *ApJ*, 512, L99
 Gao, Y., & Solomon, P. M. 2004a, *ApJS*, 152, 63
 Gao, Y., & Solomon, P. M. 2004b, *ApJ*, 606, 271
 Genzel, R., Baker, A. J., Tacconi, L. J., Lutz, D., Cox, P., Guilleaume, S., & Omont, A. 2003, *ApJ*, 584, 633
 Graciá-Carpio, J., García-Burillo, S., Planesas, P., Fuente, A., & Usero, A. 2008, *A&A*, 479, 703
 Greve, T. R., et al. 2005, *MNRAS*, 359, 1165
 Greve, T. R., Hainline, L. J., Blain, A. W., Smail, I., Ivison, R. J., & Papadopoulos, P. P. 2006, *AJ*, 132, 1938
 Handa, T., Nakai, N., Sofue, Y., Hayashi, M., & Fujimoto, M. 1990, *PASJ*, 42, 1
 Helfer, T. T., Thornley, M. D., Regan, M. W., Wong, T., Sheth, K., Vogel, S. N., Blitz, L., & Bock, D. C.-J. 2003, *ApJS*, 145, 259
 Heyer, M., Krawczyk, C., Duval, J., & Jackson, J. M. 2009, *ApJ*, 699, 1092
 Hopkins, P. F., Murray, N., Quataert, E., & Thompson, T. A. 2010, *MNRAS*, 401, L19
 Isaak, K. G., Chandler, C. J., & Carilli, C. L. 2004, *MNRAS*, 348, 1035
 Issa, M. R., MacLaren, I., & Wolfendale, A. W. 1990, *A&A*, 236, 237
 Kennicutt, R. C., Jr. 1998, *ApJ*, 498, 541
 Kennicutt, R. C., Jr., et al. 2007, *ApJ*, 671, 333
 Kennicutt, R. C., et al. 2009, *ApJ*, 703, 1672
 Kim, W.-T. 2002, Ph.D. Thesis,
 Kim, D.-C., & Sanders, D. B. 1998, *ApJS*, 119, 41
 Knudsen, K. K., Walter, F., Weiss, A., Bolatto, A., Riechers, D. A., & Menten, K. 2007, *ApJ*, 666, 156
 Kovács, A., Chapman, S. C., Dowell, C. D., Blain, A. W., Ivison, R. J., Smail, I., & Phillips, T. G. 2006, *ApJ*, 650, 592
 Kroupa, P. 2001, *MNRAS*, 322, 231
 Krumholz, M. R., McKee, C. F., & Tumlinson, J. 2009, *ApJ*, 699, 850
 Krumholz, M. R., & Matzner, C. D. 2009, *ApJ*, 703, 1352
 Krumholz, M. R., & McKee, C. F. 2005, *ApJ*, 630, 250
 Krumholz, M. R., & Tan, J. C. 2007, *ApJ*, 654, 304
 Krumholz, M. R., & Thompson, T. A. 2007, *ApJ*, 669, 289
 Laor, A., & Draine, B. T. 1993, *ApJ*, 402, 441
 Leitherer, C., et al. 1999, *ApJS*, 123, 3
 Leroy, A. K., Walter, F., Brinks, E., Bigiel, F., de Blok, W. J. G., Madore, B., & Thornley, M. D. 2008, *AJ*, 136, 2782
 Levin, Y. 2007, *MNRAS*, 374, 515
 Lisenfeld, U., & Ferrara, A. 1998, *ApJ*, 496, 145
 Martin, D. C., et al. 2005, *ApJ*, 619, L59
 Matzner, C. D. 2002, *ApJ*, 566, 302
 Mauersberger, R., Henkel, C., Wielebinski, R., Wiklind, T., & Reuter, H.-P. 1996, *A&A*, 305, 421
 McCrady, N., Gilbert, A. M., & Graham, J. R. 2003, *ApJ*, 596, 240
 McCrady, N., & Graham, J. R. 2007, *ApJ*, 663, 844
 McKee, C. F., & Ostriker, J. P. 1977, *ApJ*, 218, 148
 Michałowski, M. J., Watson, D., & Hjorth, J. 2010, *ApJ*, 712, 942
 Mirabel, I. F., Booth, R. S., Johansson, L. E. B., Garay, G., & Sanders, D. B. 1990, *A&A*, 236, 327
 Momjian, E., Carilli, C. L., Riechers, D. A., & Walter, F. 2007, *AJ*, 134, 694
 Muñoz-Mateos, J. C., et al. 2009, *ApJ*, 701, 1965
 Murphy, T. W., Jr., Soifer, B. T., Matthews, K., Armus, L., & Kiger, J. R. 2001, *AJ*, 121, 97
 Murray, N. 2010, *arXiv:1007.3270*
 Murray, N., Quataert, E., & Thompson, T. A. 2005, *ApJ*, 618, 569
 Murray, N., Quataert, E., & Thompson, T. A. 2010, *ApJ*, 709, 191
 Murray, N., & Rahman, M. 2010, *ApJ*, 709, 424
 Narayanan, D., Cox, T. J., Shirley, Y., Davé, R., Hernquist, L., & Walker, C. K. 2008, *ApJ*, 684, 996
 Neri, R., et al. 2003, *ApJ*, 597, L113
 O'dell, C. R., York, D. G., & Henize, K. G. 1967, *ApJ*, 150, 835
 Ostriker, E. C., Stone, J. M., & Gammie, C. F. 2001, *ApJ*, 546, 980
 Paumard, T., et al. 2006, *ApJ*, 643, 1011
 Rahman, M., & Murray, N. 2010, *ApJ*, 719, 1104
 Riechers, D. A., et al. 2006, *ApJ*, 650, 604
 Riechers, D. A., Walter, F., Carilli, C. L., & Bertoldi, F. 2007, *ApJ*, 671, L13
 Riechers, D. A., Walter, F., Carilli, C. L., Bertoldi, F., & Momjian, E. 2008, *ApJ*, 686, L9
 Riechers, D. A., et al. 2009b, *ApJ*, 703, 1338
 Sajina, A., et al. 2008, *ApJ*, 683, 659
 Sakamoto, K., et al. 2008, *ApJ*, 684, 957
 Sanders, D. B., Scoville, N. Z., & Soifer, B. T. 1991, *ApJ*, 370, 158
 Schinnerer, E., Böker, T., Emsellem, E., & Lisenfeld, U. 2006, *ApJ*, 649, 181
 Schinnerer, E., Böker, T., Emsellem, E., & Downes, D. 2007, *A&A*, 462, L27
 Schinnerer, E., et al. 2008, *ApJ*, 689, L5
 Scoville, N. 2003, *Journal of Korean Astronomical Society*, 36, 167
 Scoville, N. Z., Polletta, M., Ewald, S., Stolovy, S. R., Thompson, R., & Rieke, M. 2001, *AJ*, 122, 3017
 Sellwood, J. A., & Balbus, S. A. 1999, *ApJ*, 511, 660
 Semenov, D., Henning, T., Helling, C., Ilgner, M., & Sedlmayr, E. 2003, *A&A*, 410, 611
 Sirko, E., & Goodman, J. 2003, *MNRAS*, 341, 501
 Smith, B. J., & Harvey, P. M. 1996, *ApJ*, 468, 139
 Socrates, A., Davis, S. W., & Ramirez-Ruiz, E. 2008, *ApJ*, 687, 202
 Sodroski, T. J., et al. 1995, *ApJ*, 452, 262
 Solomon, P. M., Rivolo, A. R., Barrett, J., & Yahil, A. 1987, *ApJ*, 319, 730
 Solomon, P. M., Downes, D., Radford, S. J. E., & Barrett, J. W. 1997, *ApJ*, 478, 144
 Solomon, P. M., & Vanden Bout, P. A. 2005, *ARA&A*, 43, 677
 Strong, A. W., & Mattox, J. R. 1996, *A&A*, 308, L21
 Tacconi, L. J., et al. 2006, *ApJ*, 640, 228
 Thompson, T. A. 2009, *Astronomical Society of the Pacific Conference Series*, 408, 128
 Thompson, T. A., Quataert, E., & Murray, N. 2005, *ApJ*, 630, 167
 Walter, F., et al. 2003, *Nature*, 424, 406

- Walter, F., Brinks, E., de Blok, W. J. G., Bigiel, F., Kennicutt, R. C., Thornley, M. D., & Leroy, A. 2008, *AJ*, 136, 2563
- Walter, F., Riechers, D., Cox, P., Neri, R., Carilli, C., Bertoldi, F., Weiss, A., & Maiolino, R. 2009, *Nature*, 457, 699
- Weingartner, J. C., & Draine, B. T. 2001, *ApJ*, 553, 581
- Weiß, A., Neinger, N., Hüttemeister, S., & Klein, U. 2001, *A&A*, 365, 571
- Wong, T., & Blitz, L. 2002, *ApJ*, 569, 157
- Wu, J., Evans, N. J., II, Gao, Y., Solomon, P. M., Shirley, Y. L., & Vanden Bout, P. A. 2005, *ApJ*, 635, L173
- Yan, L., et al. 2010, *ApJ*, 714, 100
- Young, J. S., & Scoville, N. 1982, *ApJ*, 258, 467
- Yun, M. S., & Hibbard, J. E. 2001, *ApJ*, 550, 104